

Unusual Rheological Behaviors of Linear PE and PE/Kaolin Composite

QIYE WU,¹ XIN WANG,² WEIPING GAO,² YOU LIANG HU,² ZONGNENG QI²

¹ Qingdao Institute of Chemical Technology, 266042 Qingdao, People's Republic of China

² State Key Laboratory of Engineering Plastics, Institute of Chemistry, Chinese Academy of Science, 100080 Beijing, People's Republic of China

Received 10 November 1999; accepted 26 May 2000

ABSTRACT: The unusual flow behaviors of linear PE melts are caused by high molecular weight, tight entanglements of molecular chains, and strong adsorption of the melt at the capillary wall. Especially, the extreme change of interface adsorption is followed by an unusual flow, and at the molecular level, the dynamic variety of entanglement and disentanglement between the adsorption chain near the wall and the nonadsorption chain is the cause of the extrusion pressure vibration. Ultrahigh molecular weight polyethylene (UHMWPE)/kaolin composites prepared by polymerization filling could be smoothly extruded through the capillary. Also, with increase of the kaolin content, the apparent viscosity of the composite decreased and the processability was improved. Under slip boundary conditions, the real shear rate and shear stress of the melt near the capillary wall were reduced. The viscosity descent (desorption) and the deformation energy decrease of the melt near the wall were the important preconditions to gain a steady flow in a second glossy zone. © 2001 John Wiley & Sons, Inc. *J Appl Polym Sci* 80: 2154–2161, 2001

Key words: linear PE; kaolin; composite; polymerization filling; unusual rheological behavior

INTRODUCTION

The unsteady flow of linear polymer melts with tight molecular entanglement in the capillary is one of the characters of their rheological properties.^{1–4} For example, ultrahigh molecular weight polyethylene (UHMWPE) and high-density polyethylene prepared with a metallocene catalyst (M-HDPE) are difficult to process for their unsteady flows. According to recent research results,^{5–8} these unusual flow behaviors can be interpreted as follows: (1) All the unusual flow be-

haviors of polymer melts are caused by a drastic change of the interaction between the melts and the capillary wall. Also, their intensity can be influenced by the entanglement degree of the molecular chains. (2) The molecular mechanisms of the melt slip at the capillary wall are various: When the adsorption between the melt and the capillary wall is strong, the disentanglement of adsorption molecular chains from nonadsorption molecular chains under high stress is the cause of the melt slip. While the adsorption between the melt and the capillary wall is weak, the mechanism of the wall slip of the polymer melt is desorption of the melt from the wall by stress. Figure 1 shows these two mechanisms. Although the wall slip can occur through decrease of the melt-

Correspondence to: Q. Wu.

Journal of Applied Polymer Science, Vol. 80, 2154–2161 (2001)
© 2001 John Wiley & Sons, Inc.

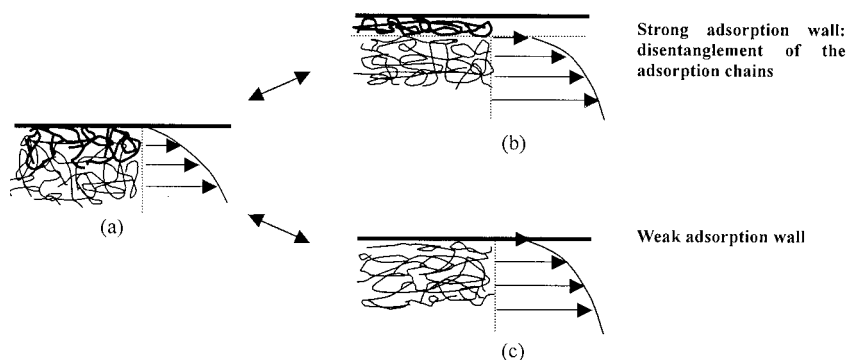


Figure 1 Two types of wall slip.

wall interaction, only the polymer melts with tight entanglement will show the wall slip and an unusual flow in a “macroscopic scale.”⁸ (3) The sharkskin on the extrudate surface is another phenomenon of unsteady flow. It is caused by the nondeterminacy of the boundary conditions of melts at the capillary exit, corresponding to the dynamic variety between entanglement and disentanglement of the adsorption molecular chains at the capillary exit.

As for UHMWPE and M-HDPE, the adsorption between melts and the metal wall of the die is very strong. These two materials have high molecular weight and very tight chain entanglement; thus, a marked pressure vibration and unusual flow of their melts by extrusion will occur and they are very difficult to process. To improve their processing flowability and mechanical properties, UHMWPE/kaolin and M-HDPE/kaolin composites were prepared by a polymerization-filling method in our work. Experiment results showed the new materials had better steady and dynamic rheological properties.^{9,10} The mechanism of the improvement is discussed in this article.

EXPERIMENTAL

The samples used for this study were powdery UHMWPE/kaolin composites with different kaolin contents prepared by a polymerization-filling method^{11,12} and pure UHMWPE produced by the same catalyst system under the same polymerization conditions. The original kaolin particle that we used in the polymerization filling are aggregates of junior particles. The BET area is about 12 m²/g and the average diameter is about 1 μm. The

diameters of more than 90% of kaolin aggregates are less than 20 μm.

The preparation procedure of UHMWPE/kaolin composites is as follows:

1. Activation of kaolin particles.

A fixed amount of TiCl₄ was added to a suspension of kaolin in hexane under nitrogen, stirred at 60°C for 3 h, then filtered off, washed thoroughly with hexane, and dried in a vacuum to gain activated kaolin. As a supported catalyst, the size of activated kaolin decreased in the polymerization-filling process. We provide TEM images of the UHMWPE/kaolin composites with various kaolin contents in Figure 2. The TEM samples were prepared by the solvent-film method. TEM photos show change of the kaolin aggregate's size.

2. Ethylene polymerization on the surfaces of kaolin.

Polymerization of ethylene was carried out in a 3-L steel autoclave at 60°C under a total pressure of 8 × 10⁵ Pa, with AlEt₂Cl/MgPh₂ as a cocatalyst (molar ratios: Al/Ti = 30; Al/Mg = 2). A prescribed amount of activated kaolin was added into the autoclave, which had been full of ethylene. After the injection of the cocatalyst, polymerization started. Samples with different kaolin contents were obtained by regulating the polymerization duration. The pure UHMWPE was prepared by the same catalyst system and under the same polymerization conditions except for the absence of kaolin.

The molecular weight was determined with the viscosity method: Use 3 g of the PE/kaolin composite, extract it for 20 h in decalin, deposit it with alcohol, filtrate and wash the extraction, dry

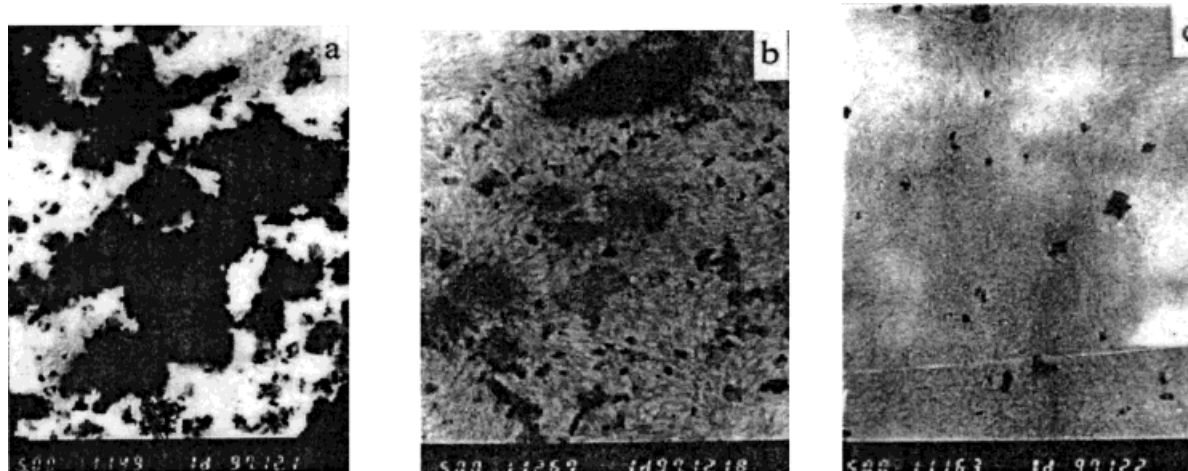


Figure 2 TEM images of UHMWPE/kaolin composites via polymerization filling. Kaolin content: (a) 70.4 wt % (b) 44.0 wt %; (c) 20.0 wt %.

in a vacuum at 60°C, and obtain the solid. This solid's intrinsic viscosity was determined at 135°C by an AVS-300-type automation viscometer after being solved by decalin. The \bar{M}_w of PE extracted from the composites was calculated from following equation¹³ and is shown in Table I: $[\eta] = 6.77 \times 10^{-4} \bar{M}_w^{0.67}$.

The capillary extrusion experiment was carried out on an Instron 3211 piston-driven capillary rheometer (a rate-constant-type rheometer). The capillaries with various L/D ratios were used: 20, 40, and 60. It was found that only a relatively narrow temperature zone was suitable for the extrusion. Higher temperature had no effect on the successful extrusion of the composites, which is similar to the cases in processing UHMWPE with the plunge-sinter method.⁵ The temperature of 270°C was chosen for the extrusion experiment. The rheology data obtained under nonslip boundary conditions was under Bagley correction and Rabinowitsch correction.

Table I Molecular Weight of UHMWPE Matrix of the Composites

Samples	Average Molecular Weight \bar{M}_w ($\times 10^6$)
Pure UHMWPE	1.50
UHMWPE/kaolin = 95/5	1.42
UHMWPE/kaolin = 90/10	1.34
UHMWPE/kaolin = 76/24	1.24

A DSR-200 rheometer in the dynamic mode with parallel-plate geometry was used in the dynamic rheology test. The experiment was carried out at 270°C, corresponding to the capillary extrusion test conditions. The sample powder was placed on the lower plate and then the upper plate was loaded down to the powder with a 1-mm gap left between the two plates. After the sample powder was heated for 30 min, the dynamic test was started with a frequency ranging from 1 to 3×10^2 Hz. Before the rheological test, 1 wt % of Antioxidant-Irganox 1010 was added to the composites to ensure no degradation at high temperature during the rheology test.

RESULTS AND DISCUSSION

Melt Fracture Under Low Shear Rate

UHMWPEs were difficult to process in the experiment. Their melts flowed unsteadily under a lower shear rate. Because of the pressure vibration and sharkskin, no steady rheological data, which accords with the viscous boundary condition, could be obtained. The flow curves of pure UHMWPE and the UHMWPE/kaolin composite are shown in Figures 3 and 4. The curves could be divided into three regions: the common viscous-elastic flow zone, the pressure-vibration zone, and the second glossy zone, where the pressure-vibration zone was, in fact, a empty region because no steady data could be obtained there.

We can see that a common viscous-elastic flow zone was absent for pure UHMWPE and the com-

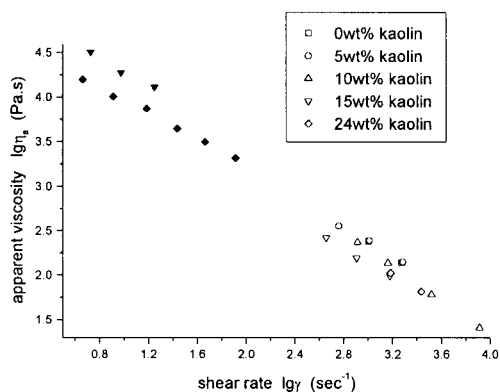


Figure 3 Apparent viscosity–shear-rate curves of UHMWPE/kaolin composites.

posites with a kaolin content <10 wt %. The stress vibration started at a low shear rate with a coarse surface of the extrudate. As the shear rate increased to a certain degree, where the second glossy zone is available, a steady stress appeared and the surface of the extrudate became better. According to Wang's idea, this phenomenon was attributed to the ultrahigh molecular weight of UHMWPE, tight entanglement of the molecular chains, and strong interaction between the polymer melt and the capillary wall (strong adsorption). Pressure vibration was the cause of the drastic change of the interaction at boundary. At the molecular level, the dynamic variety of entanglement and disentanglement between the adsorption chain and the nonadsorption chain near the capillary wall was the cause of the pressure vibration.⁵ Also, the high elasticity of the melt was another cause for the unusual flow of the melt.¹⁴

Similar to UHMWPE, HDPE prepared with the metallocene catalyst (M-HDPE) could also flow unsteadily at a low shear rate.¹¹ On the contrary, HDPE prepared with a Ziegler–Natta catalyst has a far weaker tendency to flow unsteadily when average molecular weights of two kinds of HDPE are the same. As known, HDPE prepared with a Ziegler–Natta catalyst has a wider distribution of molecular weight and its chain entanglements are fewer. When the melt is extruded through a capillary, the ingredients with low molecular weight will tend to migrate to the capillary wall. Thus, the adsorption strength between the melt and the capillary wall can be decreased.

It should be noticed that the tendency of melts to flow unsteadily could be weakened by increasing the kaolin content in the UHMWPE/kaolin

composites prepared by the polymerization-filling method. The melt of the composites with a kaolin content >15 wt % behaved like a normal polymer melt and could be extruded at a low shear rate. The composites had whole flow curves composed of the common viscous-elastic flow zone, the pressure-vibration zone, and the second glossy zone. It was also found in Figures 3 and 4 that the more kaolin content there is in the composites the lower is the apparent viscosity. This phenomenon proved that the processability of the composites was improved by the addition of kaolin with the polymerization-filling method.

As a common rule, the addition of inorganic fillers will increase the viscosity of a composite system,^{14,15} and the more filler that is added, the higher the viscosity will become. On the contrary, UHMWPE/kaolin composites prepared by the polymerization-filling method showed a different rheological property. Thus, the addition of inorganic fillers by the polymerization-filling method can be a new way to improve the processability of UHMWPE and other polymers with high molecular weight and tight chain entanglements.

The polymerization-filling method is different from the melt-mixing method.^{16–23,26} In brief, it provides excellent interface adhesion (part of which may be chemical links) or wettability between inorganic fillers and PE molecular chains, which was shown in our extraction result. A relatively large amount of PE remained after extraction for UHMWPE/kaolin composites via polymerization filling. A similar phenomenon was reported in the literature.²⁴ There is a little PE left after extraction for the composites via melt-mixing. The excellent interface adhesion or wettability leads to a decrease of molecular chain flexibility and to a decrease of the chain entanglements. The decrease of the chain entanglements will re-

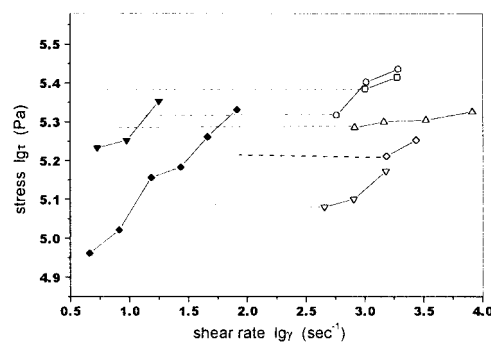


Figure 4 Stress–shear-rate curves of UHMWPE/kaolin composites.

sult in a decrease of the elasticity of the melts. On the other hand, the presence of filler particles can also weaken the adsorption strength between the molecular chain and the capillary wall. Then, the unusual flow of the melt in a “macroscopic scale” is more difficult to take place and the melt can easily flow through the capillary.

Moreover, the excellent interface adhesion or wettability will ensure that the dispersion of kaolin particles in the matrix is unalterable; then, the uniform structure of the melt can be obtained. Therefore, the melt fracture caused by the melt matrix difference will be eliminated. Moreover, with decrease of the adsorption strength between the melt and the capillary wall, the surface of the extrudate can be improved and the possibility of melt fracture becomes small. In the experiment, it was discovered that the more particles added the more remarkable these above effects were.

Slip-boundary Condition Under High Shear Rate

As shown in Figures 3 and 4, the pressure vibration of the UHMWPE melt and the UHMWPE/kaolin composites will take place when the shear rate is low. But in a higher shear-rate zone, namely, the second glossy zone, all melt samples will begin to flow steadily with a smooth extrudate surface. In this zone, the melt may be continuously slipped on the capillary wall; then, the slip boundary condition is available. We can see in Figure 4 that the melt stress near the wall is low while the shear rate there is high in the second glossy zone.

As is well known, by a capillary rheometer, only the viscosity of the melt near the capillary wall can be measured and the method to analyze the data obtained from the capillary rheometer is based on the viscous (nonslip) boundary-condition hypothesis.²⁵ Now, the nonslip boundary condition is not present in the second glossy zone; consequently, the stress and shear rate calculated with the mentioned method cannot stand under the real conditions. It is necessary then to examine the slip boundary condition at the high shear-rate zone.

Shear Stress Near the Wall Under Slip Boundary Condition

For an arbitrary segment of the melt in the capillary, as in Figure 5, all external forces on the segment should be equivalent when the segment flows steadily. There are two external forces: the

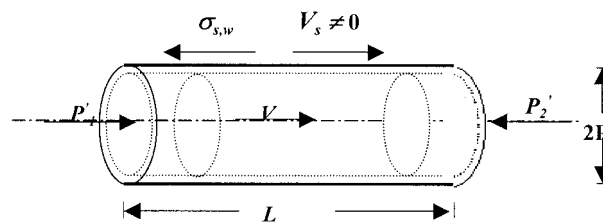


Figure 5 Calculation of the shear stress near the wall.

pressure difference between the two top surfaces of the fluid cylinder and the friction resistance on the side face of the cylinder. Two forces should be equivalent:

$$\begin{aligned} \pi R^2 \Delta P &= f = \sigma_{s,w} 2\pi R L \\ \therefore \sigma_{s,w} &= \frac{R \Delta P}{2L} \end{aligned} \quad (1)$$

This result is well known: The equation is valid for Newtonian fluid and non-Newtonian fluid, and now it is also valid under slip boundary conditions, where $\sigma_{s,w}$ is the moving friction stress on the capillary wall. It is equal to the shear stress on the melt near the capillary wall in this case.

It is surmisable that the wall resistance on the melt is static friction under a viscous boundary condition. When the flow speed becomes greater and the deformation energy of the melt near the wall is accumulated enough to overcome the maximum static friction, then the melt should slip along the capillary wall and the wall resistance should be moving friction. The deformation stress of the melt near the wall in the slip boundary condition should be smaller than is the stress in a viscous boundary condition, because the moving friction is smaller than is the maximum static friction. Then, a lower pressure difference and a lower shear stress near the wall should be measured, when the rheological measurement is carried out by a rate-constant-type rheometer as in Figure 4. On the other hand, if the measurement is carried out by a pressure-constant-type rheometer, the volume flux should increase so that the shear rate calculated from volume flux should increase.

As for the UHMWPE melt slipping along the capillary wall, it is obvious that the decrease of the viscous resistance near the wall is caused by the abrupt decrease of the molecule interaction at the interface. The molecular mechanism shown is

the disentanglement between absorption molecular chains near the wall and nonabsorption chains, as shown in Figure 1 (strong adsorption wall), that is, the disentanglement leads to form one very thin melt layer with a relatively low viscosity near wall; thereby, desorption of the melt can take place. As is well known, desorption is one of the important preconditions to obtain a steady slip boundary at the wall.⁵ Once desorption occurs, the unsteady flow should be restrained and the second glossy zone can exist.

Shear Rate Near The Wall Under Slip Boundary Condition

The calculation of the shear rate for the rheometer is based on the measurement of the volume flux. Due to the complication of calculation for a non-Newtonian fluid, we suppose that the polymer melt is a Newtonian fluid.

Similar to the velocity-distribution formula in the capillary under the viscous boundary condition,¹⁵ it follows under the slip boundary condition that

$$V_z = V_s + \frac{1}{4} \frac{1}{\eta_0} \frac{\partial P'}{\partial z} (R^2 - r^2) \quad (2)$$

where V_s is the slip speed of melt on the wall; $\partial P'/\partial z$, the pressure gradient in the capillary under the slip; and η_0 , the melt viscosity. We discuss hereinafter the equation's meanings in both cases of a pressure-constant-type rheometer and a rate-constant-type rheometer.

Pressure-constant-type Rheometer. The difference between the velocity distribution formula under the slip boundary condition and the one under the viscous boundary condition lies only in the contribution of the slip speed, but the curvature of parabola-type velocity-distribution curve remains, as shown in Figure 6(a), when the pressure gradient is the same. It is obvious that the volume flux under the slip boundary condition is larger than that under the viscous boundary condition. In the case when the formula for the calculation of shear rate from the volume flux was still introduced, then

$$\frac{\dot{\gamma}_{\text{slip}}}{\dot{\gamma}_{\text{vis}}} = 1 + \frac{4b_c}{R} \quad (3)$$

This equation means that the shear rate near the wall under the slip boundary condition is larger

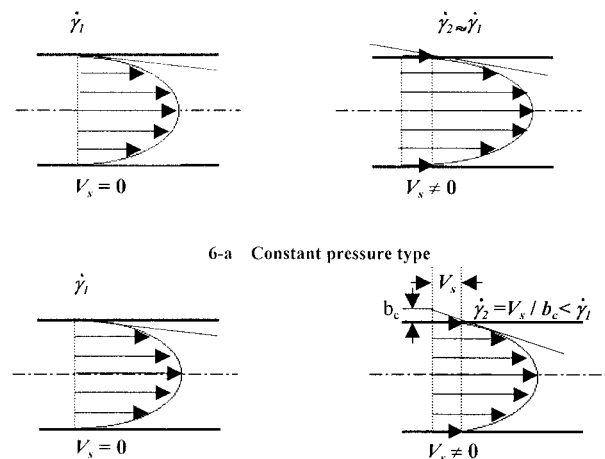


Figure 6 Velocity distribution curves in the capillary.

than that under the viscous boundary condition: ($\dot{\gamma}_{\text{slip}} > \dot{\gamma}_{\text{vis}}$). The difference depends on the value of the capillary diameter R and b_c , where $b_c = V_s/\dot{\gamma}_{\text{vis}}$ is called as the extrapolation length at the transit point on the boundary,⁸ as shown in Figure 6. But the conclusion, $\dot{\gamma}_{\text{slip}} > \dot{\gamma}_{\text{vis}}$, is unavailable from a slope variety of the velocity curve at the wall in Figure 6(a). Therefore, we can say that the pressure-constant-type rheometer is not fit for the study of the shear rate under the slip boundary condition.

Rate-constant-type Rheometer. There is a great difference between the velocity distribution curve under the slip boundary condition and that under the viscous boundary condition, when pulsive speeds of the piston are the same. Because the melt slips at the wall, the velocity curve shape becomes blunter and the curvature of the parabola becomes smaller when the volume flux remains constant [Fig. 6(b)]. It is apparent that the extrapolation length b_c becomes larger and the real shear rate near the wall becomes smaller in this case. It is known from eq. (2) that the curvature of the parabola becomes smaller primarily due to decrease of the coefficient value $1/4 (1/\eta_0) [(\partial P')/(\partial z)]$. Also, because the phenomenon of “wall slip” is not constitutive in principle, then the decrease of the coefficient is caused mainly by decrease of the pressure fall between the two tops of the capillary, $\partial P'/\partial z$, which means that the shear stress at the capillary wall decreases in the slip boundary condition. This is shown clearly in eq. (1) and in the measurement results in Figure 4. We think, in this case, that the melt viscosity measured is only the viscosity of the melt in the

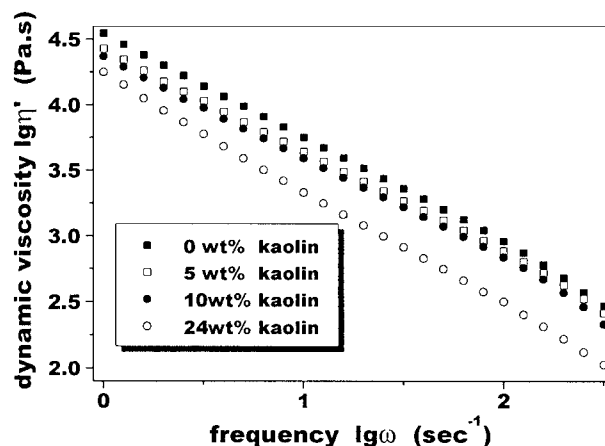


Figure 7 Dynamic viscosity of UHMWPE/kaolin composite at 270°C.

gap between the capillary wall and the melt mainstream. The viscosity of the melt mainstream in the capillary cannot be measured by the common capillary rheometer, due to that the calculation of the shear rate is not valid under the slip boundary condition.

In summary, the real shear rate of the melt near the wall should decrease and the shear stress should also decrease when the boundary condition between the melt flow and the capillary wall transits from the viscous boundary condition to the slip one in the second glossy zone. The elastic deformation energy absorbed by the material as well as the real viscoelastic deformation of the material in a high-speed flow should decrease, so the melt fracture due to the accumulation of elastic energy is restrained. This is one of the reasons to obtain a steady slip flow in the second glossy zone.

Viscoelastic Behavior in Dynamic Rheological Measurement

The relationship between the dynamic viscosity η' and the vibration frequency ω of UHMWPE/kaolin composites is shown in Figure 7. Similar to the apparent viscosity, the dynamic viscosity decreased with increase of the kaolin content. Both the results of the dynamic rheological test and the steady rheological test proved that the kaolin fill could improve the rheological property of the composites.

The linear PE melt with a high molecular weight is distinct from common polymer melts for its high elasticity. It is the physical entanglement of molecular chains that leads to the high elastic-

ity of the melt, and the entanglement cannot be eliminated by high temperature. One way to reduce the elasticity is to add inorganic fillers to the composite system, especially in the polymerization-filling method. As shown in Figure 8, the storage modulus and loss modulus of UHMWPE/kaolin composite melts decreased with increase of the kaolin content in the experimental frequency range.

It is obvious that kaolin introduced in the polymerization-filling method can reduce remarkably the elasticity of the melt of UHMWPE. The reason is in the "chemical links" existing between the kaolin particles and the PE molecular chains. The "chemical links" make the motion of molecular chain difficult; then, the elasticity of the melts decrease. Moreover, kaolin is an inorganic filler without high elasticity. In short, decrease of the melt elasticity is attributed to a lower flexibility of molecular chains and less chain entanglement, which are caused by the excellent interface adhesion between kaolin particles and PE molecular chains.

CONCLUSIONS

1. The unusual flow of linear PE is caused by its high molecular weight, tight entanglements of molecular chains, and strong adsorption between the melt and the capillary wall. Especially, the extreme change of interface adsorption is followed by an unusual flow, and at the molecular level, the dynamic variety of entanglements and disentanglements between the adsorption chain near the wall and the nonadsorption

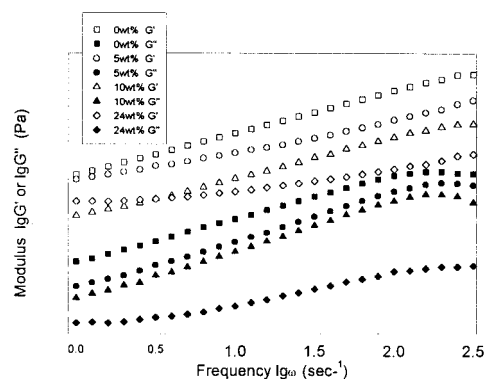


Figure 8 Storage modulus and loss modulus of UHMWPE/kaolin composites at 270°C.

- chain is the cause of the extrusion pressure vibration.
2. The UHMWPE/kaolin composite prepared by the polymerization-filling method could be successfully extruded through the capillary. This may be attributed to the decrease of entanglement points and weaker adsorption between the melt and the capillary wall, which was caused by excellent interface adhesion (part of which may be chemical links) or wettability between the inorganic fillers and the PE molecular chains.
 3. In the second glossy zone where slip boundary conditions are present, the real shear rate and shear stress of the melt near the capillary wall are lower than are those shown by a common rule for flow curves. The decrease of the viscous effect near the capillary wall (desorption) and the lower elastic deformation energy of the melt are the important preconditions to obtain a steady slip flow in the second glossy zone.
 4. The dynamic viscosity and storage and loss moduli of UHMWPE/kaolin composites prepared by the polymerization-filling method could be reduced by the addition of kaolin particles.

REFERENCES

1. Denn, M. M. *Annu Rev Fluid Mech* 1990, 22, 13.
2. Larson, R. *Rheol Acta* 1992, 31, 213.
3. Kalika, D. S.; Denn, M. M. *J Rheol* 1987, 31, 815.
4. Hatzikiriakos, S. G.; Dealy, J. M. *J Rheol* 1992, 36, 845.
5. Wang, S.Q. In *Advantage of Oversea's Polymer Science*; He, T.; Hu, H., Eds; Chemical Industry: Peking, 1997; Chapter 14.
6. Wang, S. Q.; Drda, P. A. *Macromolecules* 1996, 29, 2627.
7. Wang, S. Q.; Drda, P. A.; Inn, Y. W. *J Rheol* 1996, 40, 875.
8. De Gennes, P. G. *C R Acad Sci Paris B* 1979, 288, 219.
9. Wang, X.; Dong, J.; Wu, Q.; Hu, Y.; Qi, Z., *J Qingdao Inst Chem Tech*, in press.
10. Wang, X.; Dong, J.; Wu, Q.; Hu, Y.; Qi, Z., *J Qingdao Inst Chem Tech*, in press.
11. Dong, J.; Hu, Y.; Qi, Z. *China Synth Res Plast* 1997, 14(2), 50–53.
12. Dong, J. Y.; Wang, X.; Hu, Y. L.; Qi, Z. N. *J Appl Polym Sci*, in press.
13. Francis, P. S.; Cooke, R. C.; Elliott, J. H. *J Polym Sci* 1958, 31, 453.
14. Han, C. D. *Rheology in Polymer Processing*; Academic: New York, 1976.
15. Wu, Q.; Wu, J. *Introduction to Polymer Rheology*; Chemical Industry: Peking, 1996.
16. Kostandov, L. A.; Enikolopov, N. S. *USSR Patent* 763 379, 1976; *Byul Izobr* 1980, 34, 129.
17. Gorelik, V. M.; Shesternina, L. A.; Borisova, L. F.; Sergeev, V. I.; Fushman, E. A. *Plast Massy* 1990, 4, 11–13.
18. D'yachkovskii, F. S.; Novokshonova, L. A. *Uspekhi Khimii* 1984, 53, 200–222.
19. Gorelik, V. M.; Fushman, E. A.; Topolkaraev, V. A.; D'yachkovskii, F. S.; Shesternina, L. A.; Borisova, L. F.; Sergeev, V. I. *J Appl Polym Sci* 1990, 40, 1095–1114.
20. Howard, E. G.; Glazar, B. L.; Collette, J. W. *Ind Eng Chem Prod Res Dev* 1981, 20, 429–433.
21. Pomogailo, A. D.; Torosyan, A. A.; Ivleva, I. N.; Pomogailo, A. D.; Echmaev, S. B.; Ioffe, M. S.; Golubeva, N. D.; Borad'ko, Y. G. *Dokl Akad.-Nauk SSSR* 1980, 52, 1148.
22. Ivanchev, S. S.; Dmitrianko, A. V. *Uspekhi Khim* 1982, 51, 1178.
23. Alexander, Y. M. *Adv Polym Sci* 1990, 96, 69.
24. Wang, Q.; Kaliaguine, S.; Ait-Kadi, A. *J Appl Polym Sci* 1992, 44, 1107.
25. Han, C. D. *J Appl Polym Sci* 1974, 18, 821.
26. Beloshenko, V. A.; Kozlov, G. V.; Varyukhim, V. N.; Slobodina, V. G. *Acta Polym* 1997, 48, 181.